Electronic structure and properties of pure and doped ϵ-FeSi from *ab initio* local-density theory

T. Jarlborg
DPMC, University of Geneva, 24 Quai Ernest Ansermet, CH-1211 Geneva 4, Switzerland
(Received 10 June 1998; revised manuscript received 5 January 1999)

Local-density calculations of the electronic structure of FeSi, $FeSi_{1-x}Al_x$, and $Fe_{1-x}Ir_xSi$ systems in the B20 structure are presented. Pure FeSi has a semiconducting gap of 6 mRy at 0 K. Effects of temperature (T) in terms of electronic and vibrational excitations are included. Various measurable properties, such as magnetic susceptibility $\chi(T)$, electronic specific heat $C(T)$, thermoelectric power $S(T)$, relative variations in resistivity $\rho(T)$, and peak positions in the density of states (DOS) are calculated. The feedback from vibrational disorder onto the electronic structure is found to be essential for a good description of most properties, although the results for $S(T)$ in undoped FeSi can be described up to about 150 K without considerations of disorder. Above this T, only the filling of the gap due to disorder accompanied by exchange enhancement, can explain the large susceptiblity. The overall good agreement with experimental data for most properties in doped and pure FeSi suggests that this system is well described by local-density approximation even at large T. Doped FeSi can be described quite well from rigid-band shifts of the Fermi energy on the DOS of pure FeSi. Spin polarization in Ir-doped FeSi leads to a semimetallic magnetic state at low T. [S0163-1829(99)07123-4]

I. INTRODUCTION

The FeSi system has been much studied since the early work of Jaccarino *et al.*,[1] which showed that the magnetic susceptibility and specific heat have unusually strong temperature (T) dependence. A renewed interest in this material is reflected in the large number of experimental and theoretical works that have been published in the last few years.[2–16] Part of the interest is technological. A large thermopower in combination with low resistivity and thermal conductivity of a semiconductor, could be exploited in form of a Peltier refrigerator. Experimental studies indicate that FeSi has optimal properties for this in the temperature range near 100 K, although they are not large enough for practical applications.[11] But most studies deal with the physics of FeSi, to find the reasons for its unusual properties. Much of the discussion concerns the properties at high T, where many properties cannot be explained by traditional means. At low T, resistivity $\rho(T)$ and optical measurements agree with band theory in that FeSi is a very narrow gap semiconductor, whereas the opinions diverge on what happens at large T (from $\sim$150 K and above). Most properties indicate that FeSi is metallic and exchange enhanced at large T, which seem incompatible with the gap being 4-7 mRy as obtained from the band results based on the local-density approximation (LDA).[2–7] Some recent works propose that FeSi is exotic in the sense that it cannot be described by LDA at large T, because of strong correlation, Kondo screening or Mott localization.[5–7]

Optical data agree well with LDA bands and show a gap of about 5 mRy at $T=0$, but this gap disappears already at about 200 K.[8] This work claimed also that there is a ''missing intensity'' so that the total intensity in the filled gap at large T, was not compensated by the intensity from above gap in the low-T data. This conclusion was later refuted in new measurements by Degiorgi *et al.*,[9] although the unusual disappearence of the gap made these authors propose a Mott localization. The optical data cannot be explained in simple terms of normal transition probabilities using the LDA band structure, and this inspired Fu *et al.*[6] to propose that strong correlation in the form of Kondo-like excitations causes disorder of the band structure. The large value of χ and C at large T can be modeled by very large and narrow density of state (DOS)-peaks on both sides of the gap,[1,10] but such peaks need to be much larger than, and are incompatible with, what is found from band theory.[2]

On the other hand, many properties at low T as well as in doped FeSi agree well with the band results. In addition to the resistivity and optical data as mentioned earlier, the measured thermopower[11] is very well reproduced by Boltzmann theory using LDA bands for slight hole doping.[4] Moreover, the pressure dependence of the magnetic susceptibility has been found to follow the calculated variation of the band gap.[3] Recent studies of doped FeSi conclude likewise that low-T properties are well described by LDA results, while at larger T the systems look more like what is typically seen in Kondo insulators with heavy mass features.[12]

A different picture of the FeSi system comes from LDA calculations which consider thermal disorder.[13,14] The effective DOS at E_F increases more rapidly with T than what is obtained from a Fermi-Dirac smearing only. The calculated $\chi(T)$ is in satisfactory agreement with experiment in this case,[14] and the band filling is simply a result of the thermal disorder. The DOS peaks near the gap become broadened and fill gradually the gap, much like what has been observed in angular resolved photoemission[15] and optical measurements.[8,9] Qualitatively, the effect of disorder on many DOS-dependent properties, is similar to the effect of Fermi-Dirac smearing. But the temperature scale has to be redefined. This is exemplified by the T variation of the quadrupole splitting on Fe, when it is interpreted via a Fermi-Dirac smearing of the DOS determined for the ordered lattice; a good fit to experiment was found when the temperature scale was renormalized by a factor of 10.[5]

At very low T it is likely that impurities play a role in determining the properties of pure FeSi, for instance in the

often seen upturn in χ at the lowest T. Measurements of χ, C, and ρ below about 10 K, show anomalies, which can be interpreted in terms of Anderson-localization of impurity states.[16]

The purpose of this paper is to investigate how the electronic structure and various properties are affected by the thermal disorder and doping. Part of these results have been published in shortened form,[4,13,14] while here more complete results are presented. Further, new results of Al- and Ir-doped FeSi are presented, as well as a more detailed description of the methods of calculation.

II. METHODS OF CALCULATION

A. Electronic structure

The cubic compound ϵ-FeSi has eight atoms per unit cell and its crystal structure is B20, which can be viewed as a distorted rocksalt structure.[2] The structure is fairly close packed with a ''touching sphere'' volume ratio of 62 percent compared to 64 percent for bcc. For the band calculations we use the self-consistent, semirelativistic, linear muffin-tin orbital (LMTO) method[17] with LDA potentials.[18] The basis set included up to f states for the 8-atom unit cell. Supercell calculations with 64 atoms/cell (where the basic cell is doubled in the x, y, and z direction) included s, p, and d states in the direct basis, while the f states were included only in the 3-center terms. The calculations contain the so-called ''combined correction'' terms to the overlaping spheres, but no other nonspherical potential corrections are included.

The use of standard LMTO in this paper is motivated by the fact that none of the studied properties require a ''full-potential'' method. Calculations of elastic constants in bcc and fcc metals including full-potential corrections, based on calculations of differences in total energies for different distortions, showed that these corrections were essential for the value of the elastic constants, but the effect on the DOS is hardly visible.[19] This fact is comforting here, where DOS-related properties are studied. The substantial gain in computational speed using standard LMTO instead of a full-potential method is essential when large super cells are to be studied (with a sufficient number of k points), since super cells are needed to avoid short-range periodicity for disordered cases, and for studies of dilute impurity concentrations.

T-dependent electronic excitations are included via the Fermi-Dirac function.[20] The tetrahedron method is used for the k space integrations, using 343 and 64 k points in 1/8th of the Brillouin Zone for the small and large unit cell, respectively. Many k points are needed to describe the sharp peaks in the DOS near the gap. Band crossings are not taken into account, and this explains why the DOS from the two unit cells are not identical for the ordered structure. The DOS from the 64-atom cell shows some additional ''noise'' at some energies, but the gap (and the DOS near to it) is identical as it should. The stable behavior of the DOS in the gap region, for varying numbers of k points and of basis size, is important because the properties that are studied in this paper depend directly on the DOS near the gap. No calculation of the effective mass from the second derivative of the band dispersion has been attempted because of the problem with a limited k point mesh.

Three compositions with doped FeSi were considered; Fe_4Si_3Al, $Fe_{32}Si_{31}Al$, and $Fe_{31}IrSi_{32}$, using one Ir (or Al) impurity atom per Fe (or Si) site in cells of totally 8 or 64 atoms. The lattice constants were the same as for pure FeSi, and no lattice relaxation around the impurity atoms was considered.

Two methods for the calculation of the exchange enhancement $\mathcal{S}$ are employed. Spin-polarized, self-consistent calculations are done for the 8-atom cells including the applied magnetic field H which gives the enhancement ($\mathcal{S}$) of the susceptibility. The enhancement is defined as the ratio between the self-consistent exchange splitting at E_F and the magnetic-field energy.[21] This ratio can be different at different k points and for different bands, while here it is sufficient to know the Fermi surface average of $\mathcal{S}$. Since the Fe-d DOS is the dominant DOS character near the gap (see later) it is convenient to calculate this average from the exchange splitting of the logarithmic derivative of the radial d-wave function.[4] This value agrees well with the more complicated calculation of the Fermi-surface average of the exchange splitting. This is easily understood from the fact that the exchange splitting of the potential, probed by the d-wave function at E_F, determines the band splittings. In cases with disorder there are differences in the exchange splitting of the logarithmic derivative of the d waves, so that one can define a local $\mathcal{S}$ value. There are smaller variations of the local DOS, and the relative variations of local DOS and $\mathcal{S}$ values are quite consistent with the relation between $\mathcal{S}$ and the DOS in Eq. (1), given below. Further, it turns out that the exchange splitting of the bands at E_F is close to the Fe-site average of the local $\mathcal{S}$ values, as is expected from a perturbative calculation where the contribution from Si sites is almost nonexistent because of their very low DOS.

The other method to calculate exchange enhancement is via the Stoner factor $\overline{S}$ as obtained from the paramagnetic bands. This method assumes frozen potential conditions and is less accurate than the fully self-consistent method. But the results are usually quite good and largely sufficient for a qualitative understanding of magnetic properties, and the method is very simple. Therefore, we will base much of the discussion of near magnetic properties on the simple Stoner model, and here we use the method for calculating $\overline{S}$ for compounds.[22] The relation between $\mathcal{S}$ and $\overline{S}$ is

$$\mathcal{S}=1/(1-\overline{S}), \tag{1}$$

where $\overline{S}$ is proportional to the DOS, N. This method is based on the assumptions of a spacially uniform exchange splitting, and that only kinetic and exchange energies contribute. However, in some situations also the Coulomb energy contributes,[23] and the exchange splitting in compounds is in general not uniform in each atom type, which explains why the Stoner model can be less precise than the first method. Fully self-consistent, spin-polarized calculations could not be made for all 64-atom cases, while in the computationally simpler case of 8 atoms/cell it was possible to compare the results from the two methods. In the following, when we quote a value of $\mathcal{S}$ it is the exchange enhancement calculated by the first method. When it has been determined via $\overline{S}$ and Eq. (1), it is explicitly pointed out. The term ''Stoner en-

hancement'' refers to ''exchange enhancement'' when using the Stoner model for its estimation.

The electron-phonon coupling, λ, is calculated in the rigid muffin-tin approximation (RMTA) for compounds.[24] This gives the dipole contribution to the coupling, and even if the DOS at E_F is large in the case of doping or disorder, λ will never be very large. This is because the DOS is dominated by Fe-*d* only. For instance, in the regions just below or above the gap, where E_F is located for interesting doping concentrations, the percentages of *s*, *p*, *d*, and *f* character on Fe are 1, 3, 95, and 1 in FeSi, while in bcc Nb their percentages at E_F are 3, 20, 73, and 4. This makes products like $N_p \cdot N_d$ and $N_d \cdot N_f$ larger in Nb than in FeSi, even when the total DOS per atom is similar. Such producs determine the dipolar electronic contribution to λ, and λ in doped FeSi will not become as large as in Nb. Owing to the weak ionicity of this material, it is not likely that the monopole contribution to λ should be important.

The DOS and Fermi velocitiy v_F are calculated using the tetrahedron integration method for the **k**-space summation. This permits calculations of the transport properties such as resistivity $\rho(T)$ and thermopower $S(T)$ within Boltzmann theory.[25] The resistivity is the inverse of the conductivity $\sigma(T)$

$$\sigma(T) = e^2 \tau \int N(E,T) v_F^2(E,T) \left[-\frac{\partial f(E,E_F,T)}{\partial E} \right] dE, \quad (2)$$

where N is the DOS, v_F is the Fermi velocity, f the Fermi-Dirac function, e is the electron charge, and τ is the scattering lifetime. τ is assumed to be a constant, and since its amplitude is unknown we calculate only relative variations of ρ due to variations in DOS and v_F. In the expression for the thermopower, τ is cancelled so that an absolute value can be calculated.

$$S(T) = e\tau T^{-1} \int (E - E_F) N(E,T) v_F^2(E,T) \times \left[-\frac{\partial f(E,E_F,T)}{\partial E} \right] dE / \sigma(T). \quad (3)$$

The meaning of the T dependence in the DOS (and v_F) will be explained in the next section, where changes in $N(E)$ due to thermal disorder are considered. In principle, one should have a smooth, continous evolution of this T dependence. However, only a limited number disordered configurations can be considered because of the large computational effort, and there will be statistical fluctuations in the T dependence of transport properties and χ, when these properties are calculated from sets of varying disorders. Therefore, we present often results that are based on a fixed DOS, and the effects of disorder are discussed qualitatively.

B. Thermal disorder

An interesting range of T is when a large part of the phonon spectrum has been occupied, so that acoustic as well as optical modes are present. The phonon spectrum can be obtained by a diagonalization of the dynamical matrix for all **q** vectors, giving phonon energies and phonon wave vectors at all sites. However, the primary interest for the feedback onto the electronic structure is due to the amplitudes of vibrations rather than the phonon energies. Therefore, one can proceed more simply and avoid a full phonon calculation, by considering the vibrational energy of individual sites.

The harmonic approximation considers a parabolic potential well for atomic vibrations. The potential energy $U = 0.5Ku^2$ is characterized by a force constant K, where u is the displacement, and the kinetic energy is $0.5M(du/dt)^2$. The sum of time averages of these two energies is constant, Ku^2. Putting this equal to the thermal energy k_BT, and adding three such oscillators (three-dimensions) give $3k_BT = Ku^2$, where $u^2 = u_x^2 + u_y^2 + u_z^2$. The relation between the averaged u and T becomes

$$\langle u^2 \rangle = 3k_BT/K, \quad (4)$$

where the force constant $K = M\omega^2$ depends on the averaged phonon spectrum rather than on the Debye frequency ω_D. This relation can be obtained from the high-T expansion of the proper phonon relations as long as one characteristic force constant is representative for the vibrations, and as long as T is small enough so that the movements of neighboring atoms are uncorrelated.[26] It is also known that this leads to a Gaussian distribution function for u with a certain mean-square displacement $\sigma^2 = \langle u^2 \rangle$.

$$g(u) = \left(\frac{1}{2\pi\sigma^2} \right)^{3/2} e^{-u^2/2\sigma^2}. \quad (5)$$

The next term in the high-T expansion for $\langle u^2 \rangle$ is only $\frac{1}{36}$ of the first term at T equal to the Debye temperature (Θ_D), and $\frac{1}{9}$ at $T = \frac{1}{2}\Theta_D$. Therefore, Eq. (4) is a reasonable approximation even at quite low T, but not at very low T when only acoustic modes are occupied.

Thus, for intermediate T, we base the estimates of u and σ on this simple scheme. The force constant is expressed in terms of Θ_D [$K = M(k_B\Theta_D/\hbar)^2$] and $\Theta_D = c\sqrt{a_0 B/M}$, where c is a structure-dependent constant. By taking into account that the calculated bulk modulus B is larger than that for most transition metals and assumimg that c is universal, one can estimate that K is larger than in typical transition metals. From this we estimate K to be about 10 eV/Å^2. This is consistent with a Debye temperature of 313 K,[16] and a reduced FeSi mass. An uncertainy of $\sim$20% in K is possible and it will rescale the temperature by the same amount.

Thermal disorder is introduced in the LMTO calculations within the unit cells containing 8 or 64 atoms, where all sites become nonequivalent as soon as disorder is introduced. Each atomic position in the unit cell is given a random displacement (but totally following the Gaussian distribution) in terms of direction and amplitude. The averaged σ^2 is calculated from all positions and T is defined from Eq. (4). Each disordered configuration represents a ''snapshot'' of the dynamical thermal disorder. The assumptions of Born-Oppenheimer conditions of fast electronic and slow vibrational-relaxation times, are likely to be valid, since the lattice stiffness of FeSi is rather normal and since the results do not depend on very slow electron relaxations. In other words, it is assumed that there is sufficient time for self-consistent electronic relaxation during the vibrational evolution in time. The self-consistent calculations include the elec-

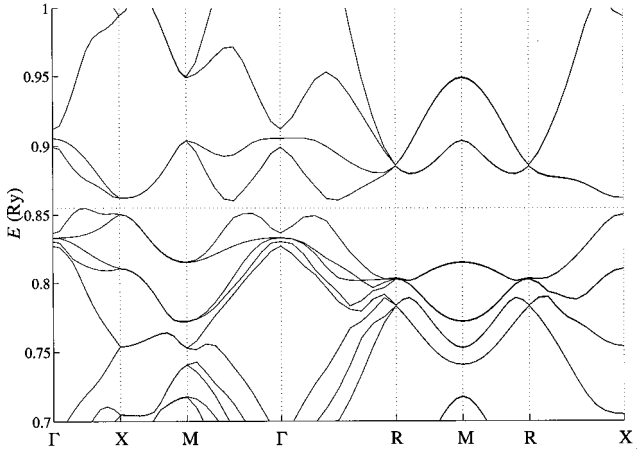

FIG. 1. The bands of ordered FeSi near the gap plotted along a few symmetry directions in the Brillouin zone. Note that the bands at ''Γ'' are calculated at a k point not exactly at (0,0,0).

tronic excitations given by the Fermi-Dirac distribution, but as was shown in Ref. 4 electronic excitations provide only a partial explanation of the T-dependent properties of FeSi.

Effects of disorder within small unit cells with different disordered configurations can be somewhat different in their details, even if the averaged $\langle u^2 \rangle$ parameter is the same. This is because of the differences in local configurations, and it can lead to variations of the details in the DOS. A more stable DOS at a given T can be composed from the superposition of the DOS from several isothermal configurations, or from the DOS of a much larger unit cell. The 64-atom calculations are very slow because of self consistency, and no spin-polarized calculations at different T and applied magnetic field were attemped for that reason. But since the closing of the gap is similar in the nonmagnetic DOS functions from 64-atom and (configuration averaged) 8-atom cases, one can be confident that the essential physics is described within the 8-atom cells.

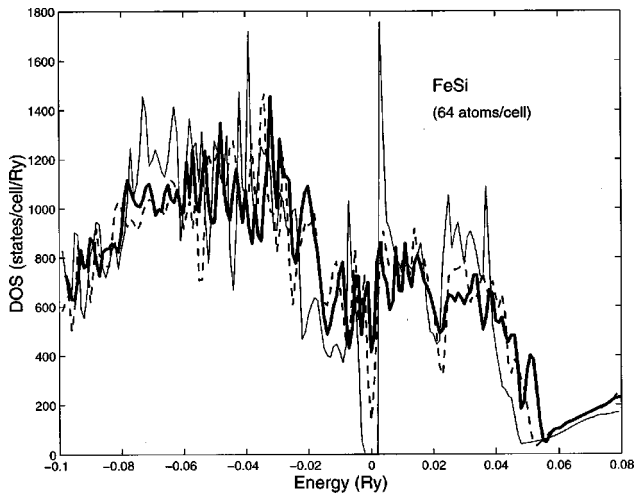

FIG. 2. Paramagnetic density of states of FeSi (64 atoms per cell) without disorder (thin line), with disorder corresponding to a temperature of about 250 K (broken line), and with disorder of about 450 K (bold line). The energy is relative to E_F.

III. RESULTS

Many results of the physical properties which rely on self-consistent spin-polarized band results are quantitatively determined for a given ideal structure. However, these results should be compared to experimental results, measured on doped FeSi at various temperatures. Therefore, in order to understand real cases, we sometimes need to extrapolate the results to non-optimal doping, using rigid band assumptions, with or without effects of thermal disorder. The discussion of magnetic properties are sometimes based on the Stoner model, which is useful but less accurate than a fully self-consistent, spin-polarized calculation. Therefore, it should be noted that the result sections contain first results for idealized super cells, but also contain a discussion of what is probable for other doping concentrations. These discussions are supported by the theoretical models rather than being quantitatively determined in all cases.

A. Band structure and density of states

The bands and the gap of FeSi at $T=0$ (no disorder) are very similar to those published earlier using different methods.[2–7] In Fig. 1 is shown the bands near the gap of undistorted FeSi along some directions. The band dispersions are very similar to those of the augmented spherical wave (ASW) method.[6] Also the full potential linear augmented plane wave (LAPW) bands of Ref. 2 are very similar except for a relative shift of two states at Γ of the order 0.2 eV below E_F, compared to the ASW or LMTO. Quantitative differences for the properties from this should be limited, since the differences in bands are localized to one part of the zone and not affecting the gap value. The calculated lattice constant $a_0=4.43$ Å is found at the minimum of the total energy E_{TOT}.[4] This is about 1% smaller than the experimental lattice constant. The bulk modulus B at a_0 is calculated to be 2.2 MBars, which is considerably larger than the experimental value, 1.3 MBars.[27] The gap E_g is indirect, ranging from 6.1 mRy at a lattice constant of 0.98 a_0 to 5.7 mRy at 1.02 a_0. This agrees well with Fu *et al.*[6] and Mattheiss and Hamann[2] who obtained $E_g=0.11$ eV (8 mRy) with the ASW and LAPW band methods, respectively, and with Christensen *et al.*[5] who obtained 0.1 eV using LMTO. The latter work noted only minor changes in the gap structure when so-called ''full-potential'' LMTO calculations were performed instead of standard LMTO. The fact that the ''full-potential'' gap is similar to the other E_g, which are based on MT-type potentials,[2,4,6,7] shows that nonspherical potentials corrections are relatively small in the B20 structure. This fact and the good agreement with the experimental gap are fortunate facts, since the computational requirement of supercell calculations with a full-potental code would have been very large and since the gap value is important for determining the T scale for many properties. The atomic sphere radii are here $0.328 \cdot a_0$ for Fe and $0.29 \cdot a_0$ for Si. This gives only small discontinuities of the potential at the limits of the spheres, but as has been noted earlier,[4,6] the gap is not sensitive to changes of sphere radii.

It can be noted that calculated band gaps in typical semiconductors like Si or GaAs are much underestimated in LDA. In such materials the ℓ character is different below and above the gap, so that there is a radial change of states from below to above the gap. As was noted above, the Fe-d

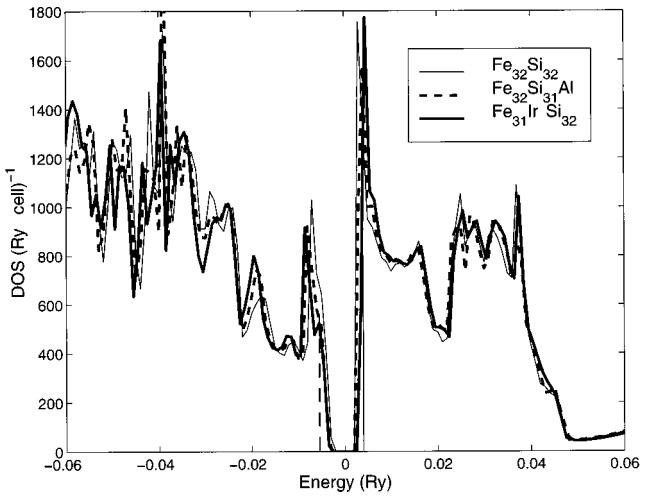

FIG. 3. Paramagnetic density of states of ordered $Fe_{32}Si_{32}$ (thin line), $Fe_{31}IrSi_{32}$ (bold line), and $Fe_{32}Si_{31}Al$ (broken line). The energy is relative to the gap center, so that the positions of E_F are indicated by the vertical-broken line for $Fe_{32}Si_{31}Al$, by the vertical line for $Fe_{31}IrSi_{32}$, and is at zero energy for $Fe_{32}Si_{32}$.

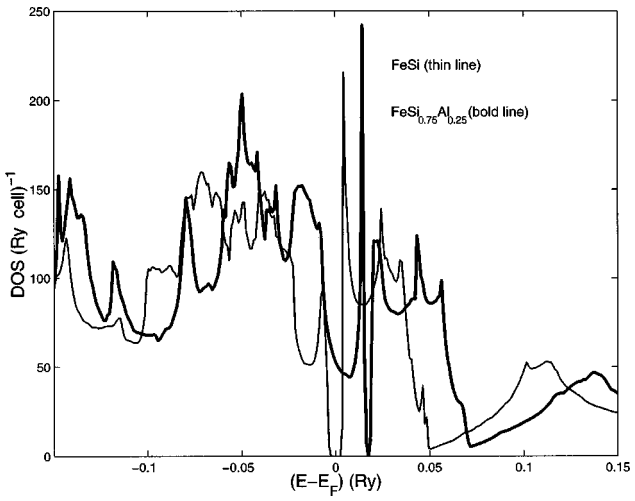

FIG. 4. Paramagnetic density of states of ordered Fe_4Si_4 (thin line) and Fe_4Si_3Al (bold line). The two curves are lined up relative to the respective position of E_F.

character is very dominating on both sides of the gap in FeSi. It might be that this similarity between an occupied ground state below the gap and an excited state above, is essential for a good LDA gap value. The widening of the gap with pressure is uncommon. This can be understood from the fact that the gap is in the middle of the Fe-*d* band. Since the band width is increasing with applied pressure it is expected that E_g increases as well. The value of $d \ln E_g / d \ln V$ is -5.9 from LMTO, which agrees roughly with the observed value.[3]

The DOS functions for ordered and disordered pure FeSi are shown in Fig. 2. The disorder is introduced as described above in the 64-atom unit cells, corresponding to a certain T. The DOS of disordered configurations in the smaller cell can be found in Refs. 14 and 20. The different results permit us to conclude that at a disorder corresponding to about 250 K, the gap is closed but still visible as a dip in the DOS. At about 450 K no trace of the gap can be seen in the DOS. This process of gap filling is essential for explaining the properties of FeSi.[14] Thermal effects due to the Fermi-Dirac smearing only, are insufficient to explain the transition of FeSi from a semiconductor at low T, to an exchange enhanced paramagnetic metal at ~ 300 K. The DOS on both sides of the gap is dominated by the Fe-*d* states. The percentage of Fe-*d* in the total DOS varies from 85-95 % in the immediate neighborhood below and above the gap. For a case with strong disorder the DOS at E_F is about 19 states/FeSi/Ry of which 16 is from Fe-*d*. This means that even if there is a sensitivity to variations in T, there are no strong charge transfers between Si and Fe sites, nor charge localization within Fe, as T is changing. However, fluctuations due to differences in local disorder make the charges to vary among different Fe sites.

Figures 3 and 4 show the DOS of pure FeSi, Fe_4Si_3Al, $Fe_{32}Si_{31}Al$, and $Fe_{31}IrSi_{32}$. The effect of doping is fairly well described by rigid-band shifts of E_F, but some details differ. Replacing a Si with Al appears to close the gap more than when an Ir replaces an iron site. The peaks in the DOS on both sides of the gap are intact despite doping and $N(E_F)$ changes rapidly with small doping concentrations. The derivative of the DOS is so large that it is even difficult to extract very precise values of $N(E_F)$. The Stoner criterion for a magnetic instability is roughly situated at 90 states per normal unit cell per Ry, so that the peak above the gap is clearly within the magnetic limit, while the peak for hole doping is just on the verge of it.

The calculated band filling and broadening of the high peak of the DOS just below the gap are in good agreement with optical measurements.[8,9] The optical conductivity showed that the gap, which is clearly visible and in agreement with the calculated gap for low *T*, is essentially filled up at $T \sim 250$ K. From the different disordered configurations we conclude that the complete filling of the gap happens around 300 K. This difference between theory and optical measurements is quite acceptable in view of the way the disorder is defined via an averaged force constant.

The peak below the gap is very narrow, ~ 3 mRy. Angular-resolved photo emission (ARPES) has been able to identify a narrow band just below the gap, which contributes to this peak.[15] It was even possible to observe a T-dependent broadening of this peak. The DOS peak below the gap is 3–4 mRy wide for the ordered case. This compares well with the bandwidth for an optimal angle in the high-resolution ARPES of 2–3 mRy, which is observed to disappear or widen to at least 10 mRy at 275 K.[15] By selecting one angle in ARPES it is possible to focus on one single band and thereby obtain a smaller bandwidth than in the DOS. Nevertheless, the peak in the calculated DOS shows a widening at higher *T*, which is consistent with the findings of the ARPES data.

B. Magnetic properties

First, we discuss the results for pure FeSi. The band broadening and the metallization are rather quick as T approaches 250-300 K. This leads to an exchange enhancement $\mathcal{S}(T)$, and the local $\mathcal{S}(T)$ (calculated from the ratio between the local-spin splitting of the potential and the applied magnetic-field energy) values are widely spread on different Fe sites. This can be understood from the spread of local disorder—at some sites the disorder is strong and may cause

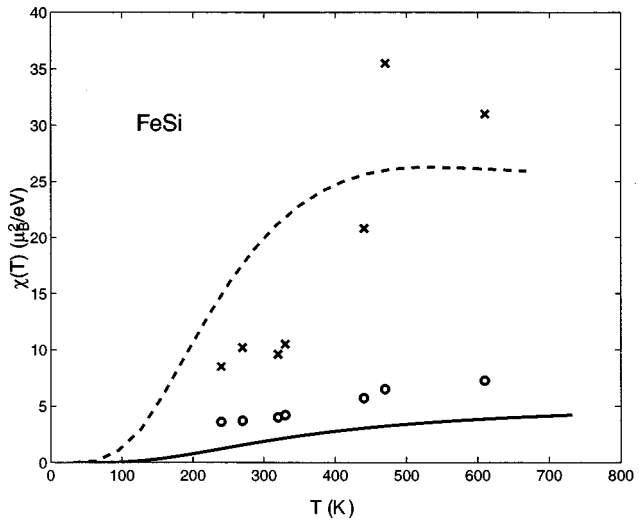

FIG. 5. Magnetic susceptibility χ for FeSi. The full line is calculated from the ordered DOS with electronic excitations only. The broken line is the result using the DOS model of Ref. 10, which closely reproduces the experimental susceptibility. Calculations using the DOS from nine different disordered configurations (corresponding to different T) using 8-atom cells, but without the $S(T)$ factors, are shown as circles. The results including the exchange enhancements $S(T)$ from spin-polarized calculations are shown as crosses.

an attractive Madelung shift of the potential. The Fermi level tends to enter into the high DOS above the (normal) gap on such sites, while on other sites E_F will be at or below the dip in the DOS. From this one can understand why the Stoner enhancement, which is sensitive to the DOS [cf. Eq. (1)], shows local variations from site to site. A striking example of local variations of DOS and enhancements, are the differences on Fe and Si sites. The DOS in disordered (or doped) FeSi is typically more than a factor 10 larger on Fe than on Si, and the Si moments in spin-polarized cases are almost zero or slightly negative.[4] As a result of this there are large differences in local exchange splittings.

The magnetic susceptibility χ can be written as

$$\chi(T)=\mu_b^2 N_{eff}(E_F,T)\mathcal{S}(T). \tag{6}$$

The effective DOS N_{eff} takes into account electronic excitations given by the Fermi-Dirac function $f(E,E_F,T)$

$$N_{eff}(E_F,T)=\int N(E,T)\left[-\frac{\partial f(E,E_F,T)}{\partial E}\right]dE. \tag{7}$$

Here E_F varies with T so that the number of electrons is conserved, and the band DOS $N(E,T)$ varies with the degree of disorder at the given T, i.e., the DOS is calculated for a disordered lattice. If $N(E,0)$ is the DOS for T=0, i.e., for a perfect lattice, and $\mathcal{S}(T)$ is 1 (no exchange enhancement), $\chi(T)$ increases from zero to about 3 μ_B^2/eV at 400 K, as in the full line of Fig. 5. The broken line in Fig. 5 is the result if $N(E)$ is given by the DOS model of Ref. 10 (two rectangular DOS functions, 5-mRy wide, 880-states/Ry/cell high, and separated by a 6-mRy gap), which is known to reproduce the experimental results. The peak heights in this model need to be so large since no exchange enhancement is included. Without the effect of DOS smearing and exchange enhancement, it is evident that the calculated DOS peaks (for $T=0$) alone are insufficient to produce the observed susceptibility. As seen in Fig. 4, the peak heights are of the order 100-200 states/Ry/cell and narrower than in the DOS model. If now the exchange enhancement is introduced, but still based on $N(E,0)$, $\chi(T)$ increases from zero at 0 K to about 4.5 μ_B^2/eV at 400 K.[4] If finally the disorder is considered so that the proper $N(E,T)$ functions are used (from different 8-atom cell configurations), and $\mathcal{S}(T)$ is an average over the enhancements of all Fe atoms (to give the global enhancement as explained earlier), χ increases further, as is shown by the crosses in Fig. 5. The susceptibility is now quite close to the experimental values.[1,10,3] The scattering of different points reflects the fact that the degree of disorder can be more or less pronounced in a small unit cell even if the u parameter is the same.

The local $\mathcal{S}(T)$ enhancements calculated for the cases with largest disorder, varies from 3.5 to 6. This is not far from the enhancement in fcc Palladium (about 7).[21,28] It can be understood from the large local (para-magnetic) DOS values, of 11-18 states/Ry/Fe-atom at this large T. This is comparable to the DOS in many transition metals, like Niobium. The very rapid variation of the DOS near the gap in (ordered) FeSi is extraordinary. Just above the gap it varies from zero to about 50 states/Ry/Fe-atom within 3 mRy. In bcc Fe $N(E_F)$ is smaller than this peak value, but clearly sufficient to put Fe beyond the limit of infinite $\mathcal{S}$.[28] This fact is important for an understanding of the unusual increase of $N_{eff}(E,T)$ when T is increased, and for the transformation of FeSi from a semiconductor at low T to an exchange enhanced paramagnet above room temperature. If a moderate electron doping is done, so that E_F enters into this high peak without causing structural instabilities or peak broadening, it seems possible to have a ferromagnetic state at low T. This possibility is investigated via the supercell calculations.

It has been proposed that spin fluctuations are responsible for the large magnetic response at large T,[29] and formation of magnetic moments at high T has been detected from neutron scattering.[30] This seems plausible in view of the spacial spread of Stoner enhancement. The variation of exchange splittings on different Fe sites supports the picture of spin fluctuations, if the disorder is so large that the local $\mathcal{S}$ tend to diverge at some region at some instance. The time scale of such fluctuations would be coupled to vibrational time scales, whereas other types of spin fluctuations need not to be related to vibrations. The calculations here did not find examples of diverging $\mathcal{S}$ or spontaneous magnetization coexisting with non-magnetic regions within the same unit cell, but it could be expected to see such cases for very large disorders.

The Stoner factors ($\overline{S}$) for the three doped cases were calculated to be 0.35, 0.47, and 1.16, for Fe_4Si_3Al, $Fe_{32}Si_{31}Al$, and $Fe_{31}IrSi_{32}$, respectively. In the former case, with a small 8-atom unit cell, it was possible to calculate $\mathcal{S}$ directly and compare the results from the two methods described in Sec. II A. In this case the Stoner factor [obtained by inverting Eq. (1)] was slightly increased to 0.43. This shows that not only the exchange and kinetic energies should determine the Stoner factor, and a full calculation slightly favors the tendency towards magnetism. Still, even with an

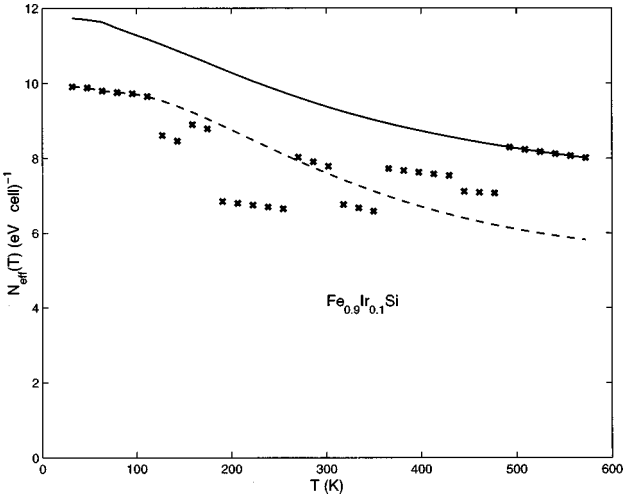

FIG. 6. Effective DOS at E_F for $Fe_{0.9}Ir_{0.1}Si$ obtained from shifting E_F to account for the Ir doping. The full and broken lines are the result using ordered and disordered (about 550 K) structures, respectively. By using panels corresponding to different intermediate disorders one obtains the crosses, where vaguely a minimum can found somewhere near 200-300 K. The effective DOS times the Stoner enhancement describes the susceptibility $\chi(T)$. Experiments show a minimum of $\chi(T)$ near 120 K (Ref. 11).

uncertainty of $\sim 15\%$ in the calculated Stoner factors for the larger cells, they predict that $Fe_{31}IrSi_{32}$, but not $Fe_{32}Si_{31}Al$, should have a magnetic transition. In terms of the DOS, a transition is likely when $N(E_F)$ per FeSi exceeds about 25 states per Ry. With this limit, it is for Al concentrations of 0.07–0.08 when the DOS peak just below the gap is close to the required height, that a magnetic transition is most probable with hole-doped FeSi. The DOS peak above the gap is higher, making magnetic transitions more likely for electron doping, if the broadening of the peaks due to strain and disorder is small as in the calculations shown here.

The measured magnetic susceptiblity of $Fe_{0.9}Ir_{0.1}Si$ was presented in Fig. 4 of Ref. 11. It has a similar shape to $\chi(T)$ in pure FeSi. However, those data had been corrected for an assumed paramagnetic iron component corresponding to 1.5% Fe, and the raw data were quoted as having a minimum at 120 K, and the amplitude of this minimum was comparable with the maximum of the susceptibility of pure FeSi. Unfortunately no other details are given concerning the uncorrected data. The calculations produce an almost magnetic state for this Ir concentration. Rigid bands, using both the FeSi and $Fe_{31}IrSi_{32}$ DOS, puts the shifted E_F just on the right-hand side of the high peak above the gap, above or near the Stoner criterion for magnetic order at $T=0$.

A calculation of the susceptibilty needs to take into account both Stoner enhancement and thermal disorder, as was concluded for pure FeSi. In the doped case this will be difficult, since the magnetic ordering, expressed by a diverging $\mathcal{S}(T)$, is so close, and spin-polarized calculations for several disordered configurations are too cumbersome. Some insight is provided by the evolution of $N_{eff}(E_F,T)$. Figure 6 shows this quantity for $Fe_{0.9}Ir_{0.1}Si$ as function of T, using rigid-band shifts on the DOS from various disordered cases. No minimum as a function of T is found when the same DOS is used over the whole T range. But when the disorder is increased, it first diminishes the DOS and than increases it again, so when $N_{eff}(E_F,T)$ is respresented by panels form various different disordered cases, as is shown by the crosses in Fig. 6, a minimum emerges somewhere around 200–300 K. The scattering of points is a result of the statistical fluctuations of disorder in small cells as mentioned earlier. The appearance of a minimum can be understood from the position of E_F on the edge of the peak for this composition, so that smearing will tend to increase the effective DOS only at the highest T. The Stoner factor will enhance the structures further. The tendency towards magnetic ordering is even more pronounced at intermediate Ir concentrations; at $x=0.04-0.05$, just above the concentration of the 64-atom unit cell, when the DOS has its maximum. It is therefore likely that the raw data mentioned in Ref. 11 represent the intrinsic behavior of $Fe_{0.9}Ir_{0.1}Si$.

One spin-polarized calculation was done for the Ir-doped, ordered supercell, $Fe_{31}IrSi_{32}$. The self-consistent calculations are very slow and only few *k* points could be used. The partially converged results indicate that the total magnetic moment is able to reach the 1 μ_B that is needed to make the supercell semimetallic for this composition, so that E_F falls in the gap for minority spins. This is at low T when the gap still is sharp. The moment is of the order 0.03 μ_B per Fe atom. This moment seems very small in view of the reasonably large Stoner factor, but it can be understood from the fact that the peak in the DOS is so narrow. At larger T, tails of the DOS will enter the gap and both the majority and minority Fermi levels are within finite DOS values. The moment can remain for some doping concentrations as long as the peak in the DOS is large.

The local variations of the magnetic moment in the Ir-doped supercell show a clear trend. Near the impurity the Fe-moments are largest, while at the most distant Fe sites, the moment is only about a third as large. Similarly, the local Fe-DOS values in the nonpolarized results are highest near the Ir site, while far from it the Fe-DOS values are smallest. The trend for an even larger super cell goes in the direction of having an electronic structure like undoped FeSi far from the impurity site, so that only the region near the impurity would become polarized. As was mentioned above, the relative variations of the local moments are larger than for the DOS, which is consistent with the relation between DOS, $\overline{S}$, and $\mathcal{S}$, given by Eq. (1). Further, the similarity of having local variations of the DOS in disordered pure FeSi and in doped FeSi, supports the idea that spin fluctuations can be coupled to vibrational disorder. However, with the cases of general disorder studied here, the local variations have no long-range correlations as in the case with the dilute impurity, and the degree of disorder is limited so that no cases of spontaneous magnetization are found.

Strong ferromagnetism is found in other transition metal silicides of the same B20 structure. MnSi, for instance, has large magnetic moments in agreement with spin-polarized band calculations[31], and the paramagnetic DOS on Mn is large to make the value of $\overline{S}$ larger than one.

Finally a comment should be made about the possibility of a metamagnetic transition. It has been argued that metamagnetism can occur as a result of strong correlation.[7] This is plausible already from the LDA results, if an applied field is able to close the gap at low T, when the DOS peaks are

sharpest.[4] The problem is that the applied field has to be very strong and that the magnetic state goes away if the field is removed, at least according to the LDA calculations. Thus the total energy seems to be lowest for the non-magnetic case, with no barrier towards a magnetic one. However, magnetic impurities can provide a field via hybridization, and this might explain the upturn in $\chi(T)$ at very low T, that is found in most FeSi samples. The case of Ir doping as mentioned above is one example of impurity-induced extended magnetism, when the impurity play the role of electron donor. Magnetic impurities with localized states act differently via their exchange splitting, and the magnetization is likely to be localized around the impurity because of the short reach of hybridization. At low T, the role of localized states in impurities will certainly influence the properties of otherwise undoped FeSi. This has been investigated experimentally by Hunt *et al.*[16] A recent experimental work studied FeSi in extremely high field, up to 450 T, at 77 K.[32] No metamagnetic transition was found, but the conductivity showed a spectacular increase for one order of magnitude when the field was increased from 200 to 450 T. These results will be discussed in Sec. III D.

C. Heat capacity

The electronic specific heat is linear in T at low temperature; $C_e=\gamma T=(\pi^2/3)k_B^2TN_{eff}(E_F,T)(1+\lambda)$, as long as the DOS has a weak T dependence. A comparison of the specific heat C_p between FeSi and CoSi revealed an ''anomaly'' in FeSi of about 3-5 J/mol/K above about 200 K. It was assumed that the vibrational part of C_p in the two compounds are identical, so that the difference should be due to electronic part only.[1,10]

The anomaly with respect to CoSi is calculated from the (electronic) kinetic energy, $\mathcal{U}$, as in the model of Ref. 10. At high T λ vanishes[26] and one obtains

$$\mathcal{U}=\int N(E)Ef(E,E_F,T)dE \tag{8}$$

and $\Delta C(T)=(d/dT)\mathcal{U}$. (The DOS of ordered structures are used, because of the problem of connecting results from different disordered configurations.) The results from the DOS of the small and large cell, are shown in Fig. 7 together with a model made to resemble the experimental data in Ref. 10, although the model parameters are different from the ones in that reference. The results follow the model quite well with a maximum not far from ~ 300 K, where the measured ΔC_p anomaly has its maximum. At large T it is expected that λ (which probably is small anyway) should decrease,[26] and this should concern the reference system as well. A possible complication is that γT for the reference system, CoSi, may show a strong nonlinear evolution at high T because of vibrational disorder. Indeed, the calculated DOS for CoSi shows that E_F is situated right at the DOS shoulder about 40 mRy above the gap, and that the effective DOS tends to increase when the DOS is broadened. However, this is only a qualitative observation; calculations of differences in C_p is difficult and the agreement with experiment shown in Fig. 7 is surprisingly good. If the DOS from a disordered configuration is used, it will increase the heat capacity more at low T, while at larger T the result is not so different from what is shown in Fig. 7.

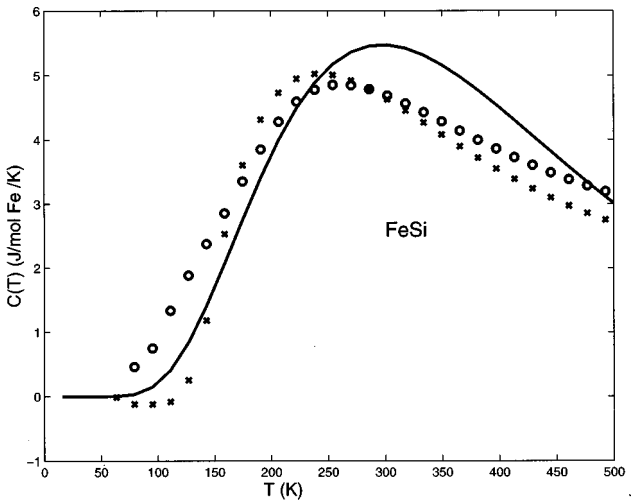

FIG. 7. Specific heat calculated from the band results for ordered structures as described in the text. The result using the DOS from the small cell is shown by the circles, and from the 64-atom cell by the crosses. The results are somewhat unstable at low T. The full line is from a DOS model made to reproduce the experimental points for $\Delta C_p(T)$ shown in Ref. 10.

It is worth noting that the DOS model made by Mandrus *et al.* to fit $\chi(T)$-data required higher and wider DOS peaks than the model made to fit $\Delta C_p(T)$.[10] The spectral weights in the DOS were 4.4 and 0.8 electrons, respectively. The difference can be interpreted as if an exchange enhancement of about 5 is included only in χ. This is consistent with our finding which has an enhancement of this order (cf. Fig. 5) in χ, but is absent in the heat capacity.

The low-T specific heat of doped $FeSi_{1-x}Al_x$ for $x=0.025$ and 0.015 was measured by DiTusa *et al.*[12] They noted a large effective mass of about 14 for the largest doping concentration. This was concluded from the large γ of about 7 and 5 mJ/mol FeK^2, for the two concentrations. The calculation for the $Fe_{32}Si_{31}Al$ supercell has a DOS of about 700 states per cell Ry, and λ is calculated in RMTA to be 0.2 for a Debye temperature of 313 K, taken from Ref. 16. Rigid band shifts of E_F on the DOS from pure 64 or 8 atom FeSi calculations do not change these estimates much. This gives $\gamma=4.6$ mJ/mol FeK^2, which is smaller than what can be extrapolated from the experimental results. Enhancement from spin fluctuations could make up for the difference since $\overline{S}$ is quite large. If E_F is adjusted in a rigid-band manner to account for $x=0.015$ one finds a reduction of γ to about 3 mJ/mol Fe K^2 (instead of 5 experimentally). Thus, the relative change in γ between the two concentrations is reflected in the sharp change in DOS between the two cases. The different amplitudes in experiment and theory can be translated into a 30–40 % lower m^* in the theory. Compared to doping of conventional semiconductors, FeSi is exceptional because of the high-DOS peaks at the gap edges. This is reflected in the large band mass of doped FeSi.

D. Transport properties

The thermopower, expressed by the Seebeck constant $S(T)$ is calculated from the band structure of ordered (very

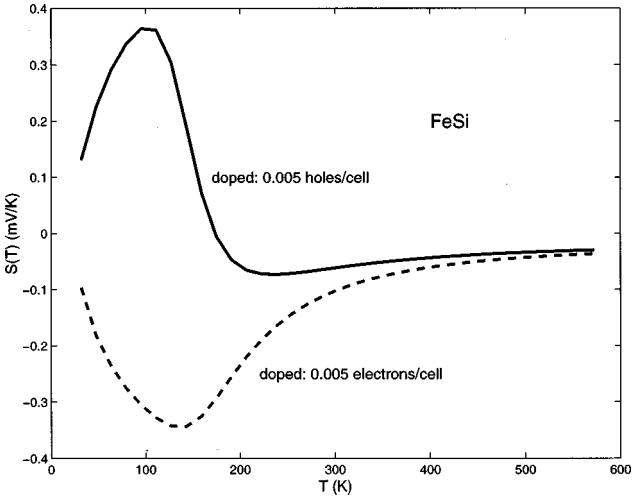

FIG. 8. The calculated Seebeck coefficient for (ordered) FeSi, where E_F has been adjusted for slight hole and electron doping, respectively. The good agreement between the hole doped case and the experimental data in Ref. 11, suggests that effects of thermal disorder are minor up to 150–200 K.

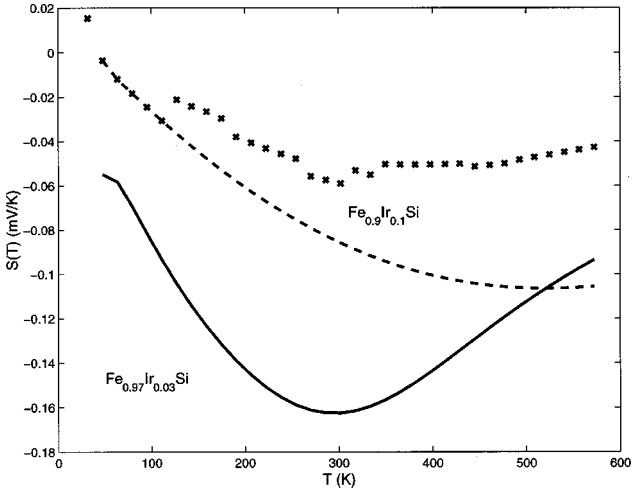

FIG. 9. The calculated Seebeck coefficient for ordered and disordered $Fe_{0.9}Ir_{0.1}Si$. The band structure is for the 8-atom cell, with E_F shifted to account for the Ir doping. The broken line is for the ordered stucture. The crosses show $S(T)$ when it is made up from different panels with different degree of disorder. Compared to the ordered case, it is seen how the minimum is displaced to lower T. The full line is for the ordered $Fe_{31}IrSi_{32}$. These results can be compared with the experimental results shown in Ref. 11 on $Fe_{0.97}Ir_{0.03}Si$: The experimental $S(T)$ curve starts at 0 at zero temperature, decreases to -0.11 mV/K at 50 K, has a wide minimum of about -0.14 mV/K near 100 K, goes up towards -0.08 mV/K at 150 K, and approches smoothly zero for $T \geqslant 250$ K.

slightly hole doped) FeSi.[4] It agrees very well with experimental data of Sales *et al.*,[11] both concerning amplitudes and T dependence up to 100–150 K.[4] The experiment is for supposedly pure FeSi, but the agreement with the calculated $S(T)$ shown in Fig. 8 suggests that there is a slight hole doping. A slight hole doping (which could even be smaller than 0.005 holes per cell) is needed to make a shift in $E_F(T)$ from near the top of the valence band at low T, to a little below the middle of the gap at high T. Exact stoichiometry implies a smaller shift of $E_F(T)$, since E_F at $T=0$ would be just at the middle of the gap, and the amplitude variation of $S(T)$ would be smaller. Doping with electrons makes a large difference, since $E_F(T)$ then shifts downwards from the edge of the conduction band to just below the midgap, as T increases, and $S(T)$ takes an opposite shape, as shown in Fig. 8.

The good agreement between experiment and theory for $S(T)$ for T up to ~ 150 K, gives an indication that effects of vibrational disorder are not very important up to this temperature, at least not for pure FeSi. $S(T)$ is small and flat for higher T, and calculations cannot distinguish clearly between different disorders.

Experimental data for Ir-doped FeSi with $x=0.03$ show a completely different $S(T)$,[11] as is expected from an electron-doped case. The calculated result, shown in Fig. 9, using the (ordered) FeSi band with E_F moved to account for the electron doping at $x=0.03$, shows a very similar shape as in the measured curve in Ref. 11, with a minimum of ~ 0.15 mV/K, except for the fact that the temperature scale is different by a factor 3 roughly. The dip in $S(T)$ is near 300 K, while near 100 experimentally. Qualitatively, it is expected that additional DOS smearing above 100–150 K, will compress the T scale, to agree better with experiment. But is is difficult to put together results from several band structures with different T-dependent disorder, to make a continous, quantitative plot of the thermopower. Nevertheless, in Fig. 9 is shown the result of $S(T)$ for $x=0.1$, when it is collected from several different disordered configurations, each one representative of the corresponding interval in T. Despite the scattering of points, it is possible to identify a minimum near 300 K, which is not found in the curve based on the $T=0$ bands only (the broken line). The amplitude agrees well with experiment, but the minimum is still at too high T. A possible explanation of this is that non rigid-band effects and spin polarization will modify the peak structures at this relatively high-doping concentration.

A similar trend concerning the peak positions, is obtained for the resistivity $\rho(T)$ in $Fe_{1-x}Ir_xSi$ for $x=0.03$, cf. Fig. 10.

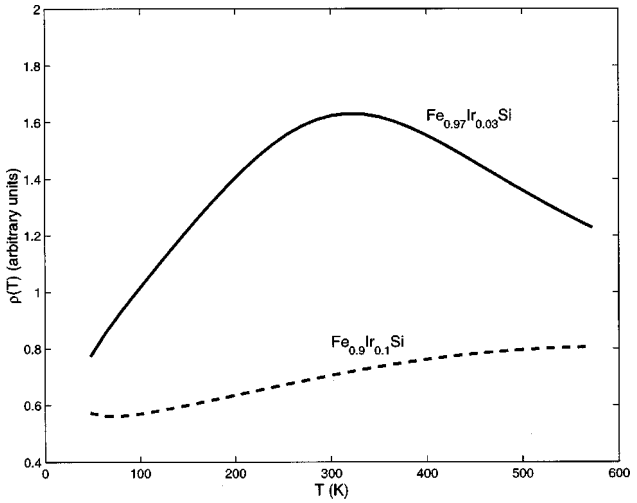

FIG. 10. Relative evolution of the resistivity in $Fe_{31}Ir\,Si_{32}$ and $Fe_{0.9}Ir_{0.1}Si$. In the latter case E_F is shifted to account for the increased Ir-doping. Experimental data in Ref. 11 show a resistivity peak at lower T.

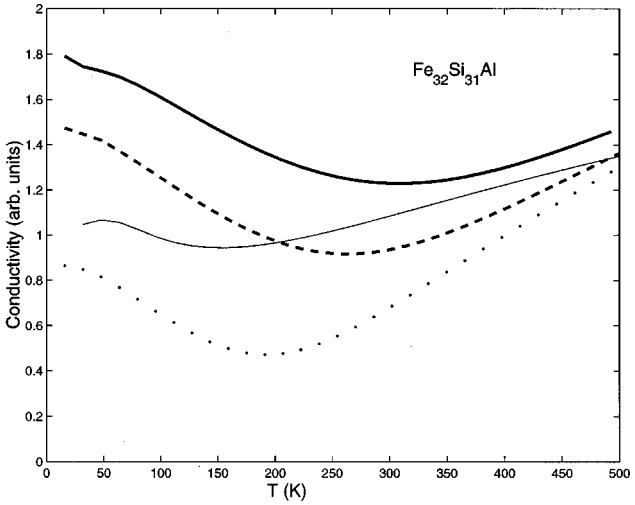

FIG. 11. Relative evolution of the conductivity in $FeSi_{0.9}Al_{0.1}$ for ordered structure (bold line), and with disorder of about 250 K (thin line). The latter agrees with the experimental data in Ref. 12, which show a conductivity minimum at about 100 K. The minimum tends to lower T, and give lower conductivity when E_F is moved closer to the gap by accounting for 0.019 (broken line) and 0.006 (dotted) holes per FeSi. In the case of ordered structure, σ tends to zero at $T=0$ when FeSi is undoped.

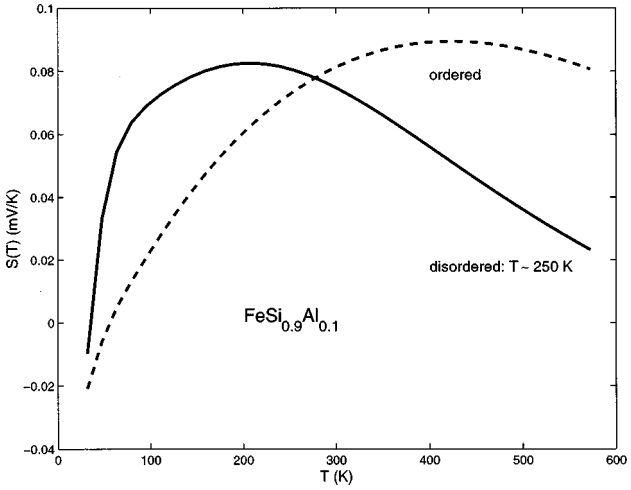

FIG. 12. The calculated Seebeck coefficient for ordered and disordered $FeSi_{0.9}Al_{0.1}$. The band structure for the 64-atom supercell containing one Al atom was used with E_F adjusted to account for the higher Al concentration. It is seen that the effect of disorder is to compress the T scale.

The experimental peak is found near 90 K,[11] while it is near 300 K from the band results. For $x=0.1$ $\rho(T)$ is increasing with T, both in the experiment and the calculation (assuming a constant life time τ), with no maximum within a wide-T range.

Measurements of the conductivity of hole-doped $FeSi_{1-x}Al_x$ with $x=0.1$ has been published by Sales *et al.*,[11] and recently within the concentration range $x=[0-0.08]$, by DiTusa *et al.*[12] The conductivity has a minimum in the T range 50-100 K when x exceeds ~ 0.05. The calculated conductivity shows the minimum, but again as in the case with electron doping, the peak position is displaced towards higher T, when the calculations are based on rigid-band shifts of E_F on the bands of an ordered structure. An example is shown in Fig. 11.

Figure 12 shows the evolution of $S(T)$ in Al-doped FeSi, with and without considerations of thermal disorder. As before, the T scale is compressed by disorder, while the experimental peak is found at even lower T for the Al-concentration $x=0.1$.[11]

Thus, pure FeSi shows very good agreement with experiment, while in the doped cases, the T scale is somewhat renormalized due to disorder. This can be understood from the fact that E_F is within the DOS at all T when the doping is important. In pure FeSi, the position of E_F is in the gap and it is not until a certain T that the band edges come close to it. Therefore, as long as E_F is within the gap region, the properties are not so sensitive to broadening due to disorder. With doping, E_F is within the DOS even at low T, and smearing has an immediate effect on the properties. This often show up as a difference in T scale in measured and calculated transport properties. On the other hand, the calculated amplitudes of $S(T)$ are always in good agreement with experiment.

A very recent experimental work of Kudasov *et al.*[32] reports a semiconductor-metal transition in FeSi in ultra-high magnetic fields. Pulsed fields as high as 450 T could be applied to FeSi at 77 K, with almost no heating. The conductivity showed a continous increase of ''approximately two orders of magnitude in a 450 T field as compared to at zero field.'' These findings can be compared to what is expected from the calculated exchange enhancement for stoichiometric, ordered FeSi of Ref. 4. At low T when thermal disorder is limited, practically no low-field exchange enhancement is expected and even a field of ~ 450 T (about 2 mRy) cannot overcome a gap of about 6 mRy. However, the findings of Ref. 32 can be understood if the sample is slightly doped and if the zero-point motion is sufficiently large to make the band egdes to extend into the gap. Then there will be some states availiable near E_F to enforce an applied field by exchange enhancement, and the material will soon approach a closed gap situation as indicated in Ref. 4. The conductivity is much enhanced in this situation, compared to the almost insulating zero field case. This mean-field mechanism for the field-induced conductivity is an alternative to the explanation via spin fluctuations as was suggested in Ref. 32, but detailed calculations using Boltzmann theory and band results for different nonstoichiometric, disordered cases are needed for a quantitative comparison with experiment. In any case, the absence of an abrupt increase of the conductivity for a particular field in Ref. 32, indicate that the semiconductor-metal transition is continous and depends on rounded off band-gap edges, rather than being the signature of a metastable transition.

IV. CONCLUSION

In conclusion, we have performed nonmagnetic as well as spin-polarized band calculations for ordered and disordered FeSi with different dopings. Various properties are calculated from the band results, and the agreement with experiment is, in general, very good. Most importantly, it has been possible to show that the unusual behavior of the suscepti-

bility can be described within LDA. Structural disorder, which can be linked to the temperature, leads to a gradual closing of the narrow gap, so that the effective DOS (per Fe) at the Fermi energy becomes comparable to that of Nb or Pd, for T larger than ~ 400 K. The increased DOS has a direct impact on the Pauli susceptibilty, and on the exchange enhancement. By taking these effects into account one obtains a $\chi(T)$ which is of the correct amplitude. This is true for the heat capacity as well, where no Stoner enhancement enters, and the calculation based on the normal DOS reproduces the essential part of the anomaly. The direct observation of bands and DOS in photoemission and optical experiments are consistent with the calculated electronic structure when disorder is considered. The transport properties are well described, except for what seems to be a somewhat too extended T scale in the case of doped FeSi. The thermopower in pure FeSi shows that thermal disorder is not crucial below ~ 150 K, for this undoped case.

Thus, as a whole we obtain a very satisfactory explanation of the properties of FeSi from LDA, provided that thermal disorder is taken into account. The band calculations are *ab initio* so the only uncertainty concerns the exact form of disorder. Despite the simplicity of the harmonic model for vibrational disorder, the band results lead even to a good quantitative description of many properties. Future work should improve the calculations of the phonon part, and larger unit cells and/or more disordered configurations are required to achieve less scatter in the calculated results. But such elaborations are not expected to modify the qualitative results very much for intermediate T. The exact behavior at the lowest T, which is not studied here, is delicate because of the relative importance of zero-point motion and low-q phonons. Different types of disorder have some influence on the results, but it is especially the difference between having disorder or not, which is most important in this paper. Thermal disorder is always present above a certain temperature, and the consequencies are particularily striking in FeSi because of its sharp DOS features near the narrow gap. These results imply that no assumptions of strong correlation are needed to explain the properties of FeSi.

ACKNOWLEDGMENTS

I am grateful to S. Dugdale for a careful reading of the manuscript and to J.F. DiTusa for sending the preprint in Ref. 12.

[1] V. Jaccarino, G. K. Wertheim, J. H. Wernick, L. R. Walker, and S. Arajs, Phys. Rev. **160**, 476 (1967).
[2] L. F. Mattheiss and D. R. Hamann, Phys. Rev. B **47**, 13 114 (1993).
[3] G. E. Grechnev, T. Jarlborg, A. S. Panfilov, M. Peter, and I. V. Svechkarev, Solid State Commun. **91**, 835 (1994).
[4] T. Jarlborg, Phys. Rev. B **51**, 11 106 (1995).
[5] N. E. Christensen, I. Wenneker, A. Svane, and M. Fanciulli, Phys. Status Solidi B **198**, 23 (1996).
[6] C. Fu, M. P. C. M. Krijn, and S. Doniach, Phys. Rev. B **49**, 2219 (1994).
[7] V. I. Anisimov, S. Yu. Ezhov, I. S. Elfimov, I. V. Solovyev, and T. M. Rice, Phys. Rev. Lett. **76**, 1735 (1996).
[8] Z. Schlesinger, Z. Fisk, H.-T. Zhang, M. B. Maple, J. F. DiTusa, and G. Aeppli, Phys. Rev. Lett. **71**, 1748 (1993).
[9] L. Degiorgi, M. B. Hunt, H. R. Ott, M. Dressel, B. J. Fenstra, G. Grüner, Z. Fisk, and P. Canfield, Europhys. Lett. **28**, 341 (1994).
[10] D. Mandrus, J. L. Sarrao, A. Migliori, J. D. Thompson, and Z. Fisk, Phys. Rev. B **51**, 4763 (1995).
[11] B. C. Sales, E. C. Jones, B. C. Chakoumakos, J. A. Fernandez-Baca, H. E. Harmon, J. W. Sharp, and E. H. Volckmann, Phys. Rev. B **50**, 8207 (1994).
[12] J. F. DiTusa, K. Friemelt, E. Bucher, G. Aeppli, and A. P. Ramirez, Phys. Rev. Lett. **78**, 2831 (1997); Phys. Rev. B **58**, 10 288 (1998).
[13] T. Jarlborg, Phys. Rev. Lett. **77**, 3693 (1996).
[14] T. Jarlborg, Phys. Lett. A **236**, 143 (1997).
[15] C.-H. Park, Z.-X. Shen, A. G. Loeser, D. S. Dessau, D. G. Mandrus, A. Migliori, J. Sarrao, and Z. Fisk, Phys. Rev. B **52**, R16 981 (1995).
[16] M. B. Hunt, M. A. Chernikov, E. Felder, H. R. Ott, Z. Fisk, and P. Canfield, Phys. Rev. B **50**, 14 933 (1994).
[17] O. K. Andersen, Phys. Rev. B **12**, 3060 (1975); T. Jarlborg and G. Arbman, J. Phys. F **7**, 1635 (1977).
[18] W. Kohn and L. J. Sham, Phys. Rev. **140**, A1133 (1965); N. D. Mermin, *ibid.* **137**, A1441 (1965); L. Hedin, B. I. Lundqvist, and S. Lundqvist, Solid State Commun. **9**, 537 (1971).
[19] P. Lerch and T. Jarlborg, Physica B **202**, 134 (1994).
[20] T. Jarlborg, Rep. Prog. Phys. **60**, 1305 (1997).
[21] T. Jarlborg and A. J. Freeman, Phys. Rev. B **23**, 3577 (1981).
[22] T. Jarlborg and A. J. Freeman, Phys. Rev. B **22**, 2332 (1980).
[23] T. Jarlborg, Phys. Rev. B **58**, 9599 (1998).
[24] M. Dacorogna, T. Jarlborg, A. Junod, M. Pelizzone, and M. Peter, J. Low Temp. Phys. **57**, 629 (1984).
[25] P. B. Allen, W. E. Pickett, and H. Krakauer, Phys. Rev. B **37**, 7482 (1988).
[26] G. Grimvall, *Thermophysical Properties of Materials* (North-Holland, Amsterdam, 1986).
[27] H. Klimker, J. M. Perz, I. V. Svechkarev, and D. G. Dolgopolov, J. Magn. Magn. Mater. **62**, 339 (1986).
[28] J. F. Janak, Phys. Rev. B **16**, 255 (1977).
[29] Y. Takahashi and T. Moriya, J. Phys. Soc. Jpn. **46**, 1451 (1979); S. N. Evangelou and D. M. Edwards, J. Phys. C **16**, 2121 (1983).
[30] G. Shirane, J. E. Fischer, Y. Endoh, and K. Tajima, Phys. Rev. Lett. **59**, 351 (1987).
[31] P. Lerch and T. Jarlborg, J. Magn. Magn. Mater. **131**, 321 (1994).
[32] Yu. B. Kudasov, A. I. Bykov, M. I. Dolotenko, N. P. Kolokl'chikov, M. P. Monakhov, I. M. Markevtsev, V. V. Platonov, V. D. Selemir, O. M. Tatsenko, A. V. Filippov, A. G. Volkov, A. A. Povzner, P. V. Bayankin, and V. G. Guk, Pisma Zh. Éksp. Teor. Fiz. **68**, 326 (1998) [JETP Lett. **68**, 350 (1998)].